Organic & Biomolecular Chemistry

PAPER

View Article Online
View Journal | View Issue

Cite this: *Org. Biomol. Chem.*, 2014, **12**, 4952

N[1,3]-sigmatropic shift in the benzidine rearrangement: experimental and theoretical investigation†

Shili Hou,‡ Xinyao Li‡ and Jiaxi Xu*

Received 11th January 2014,
Accepted 17th April 2014

DOI: 10.1039/c4ob00080c

www.rsc.org/obc

The N[1,3]-sigmatropic shift in the benzidine rearrangement has been studied in depth experimentally with the aid of density functional theory (DFT) calculations. The designed substituted *N*,*N*′-diaryl hydrazines rearrange exclusively to the expected *o*/*p*-semidines and diphenylines. Intercrossing experiments support the intramolecular rearrangement process. Radical trapping experiments exclude the intermediacy of biradicals in the rearrangements. Computational results demonstrate that the *o*-semidine rearrangement involves a novel N[1,3]-sigmatropic shift and the *p*-semidine rearrangement proceeds *via* tandem N[1,3]/N[1,3]-sigmatropic shifts, while the diphenyline rearrangement occurs through cascade N[1,3]/[3,3]-sigmatropic shifts. The proposed mechanism involving the key N[1,3]-sigmatropic shift as the rate-limiting step is in good agreement with reported kinetic isotope measurements. The combined methods provide new insight into the formation mechanism of *o*/*p*-semidines and diphenylines in the benzidine rearrangement and support the unprecedented suprafacial symmetry allowed N[1,3]-sigmatropic shift with an inversion of the configuration in the migrating nitrogen atom.

Introduction

The [1,3]-sigmatropic shift, a typical thermal pericyclic rearrangement, is a powerful strategy for the construction of biologically active molecules in synthetic organic chemistry.[1–5] The structure of the transition state and the configuration of the products from the [1,3]-sigmatropic shift have been predicted by the Woodward–Hoffmann selection rule through the suprafacial symmetry of the frontier molecular orbital approach with the inversion of the configuration in the migrating groups (Fig. 1).[6] Among them, the C[1,3]-sigmatropic shift has been widely explored experimentally and theoretically,[2] while the O/N[1,3]-sigmatropic shift has been rarely reported. Recently, we have offered mechanistic insight into the O[1,3]-sigmatropic shift in the abnormal Claisen rearrangement.[7] Now we are particularly interested in the N[1,3]-sigmatropic shift.

Acid-catalyzed benzidine rearrangements have been studied extensively over more than 150 years,[8] in which the parent *N*,*N*′-diphenyl hydrazine (**1**) gives *p*-benzidine (**2**, 70%) and diphenyline (**3**, 30%)[9,10] as the main products and some other secondary products such as *o*-benzidine (**4**), *p*-semidine (**5**), and *o*-semidine (**6**) (Scheme 1).[11] In some cases, *o*-benzidine, *p*-semidine, and *o*-semidine type products were obtained in considerable yields from certain substituted *N*,*N*′-diaryl hydrazines.

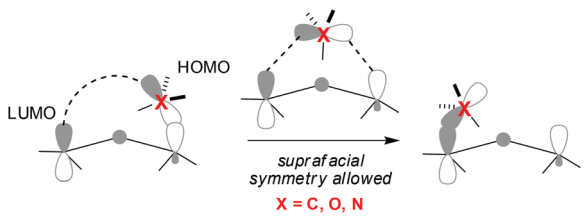

Fig. 1 Concerted [1,3]-sigmatropic shift with inversion of the configuration in the migrating group.

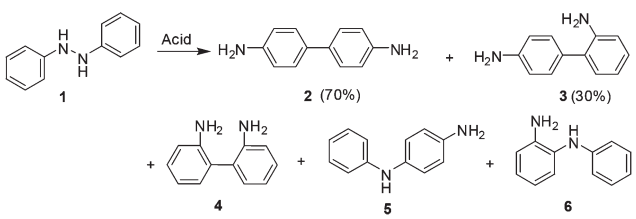

Scheme 1 Benzidine rearrangement of *N*,*N*′-diphenylhydrazine (**1**).

State Key Laboratory of Chemical Resource Engineering, Department of Organic Chemistry, Faculty of Science, Beijing University of Chemical Technology, Beijing 100029, People's Republic of China. E-mail: jxxu@mail.buct.edu.cn; Tel: +86 10 64435565

† Electronic supplementary information (ESI) available: Details of rearrangement reactions, copies of ^{1}H NMR and ^{13}C NMR spectra of products, copies of LC-MS diagrams, and computational details. See DOI: 10.1039/c4ob00080c

‡ These two authors contributed equally.

A large amount of work has been devoted to the mechanistic investigation of the benzidine rearrangements, where the controversies were concentrated on the polar transition state theory (one concerted step) and Dewar's π complex theory (two stepwise steps).[12] The question as to whether the rearrangement occurred by a stepwise or concerted mechanism remained unresolved until measurements of heavy-atom kinetic isotope effects (KIEs) were performed by Shine and coworkers.[13–15] A concerted [5,5]-sigmatropic shift was proposed on the basis of KIE results on nitrogen and carbon atoms for the formation of **2**. Furthermore, an inverse secondary deuterium isotopic effect for the disappearance of **1** supported the conclusion drawn from the nitrogen and carbon KIE results.[13b,c] In contrast, the formation of diphenyline (**3**) was characterized *via* a substantial KIE for the N atom but with a slight 2,2′,6,6′-$^{13}C_4$ KIE, in accord with an intramolecular and nonconcerted mechanism.[13c] In addition, KIE results for the formation of *o*-benzidines from *N*,*N*′-di(2-naphthyl)hydrazine and *N*-2-naphthyl-*N*′-phenylhydrazine were clearly indicative of a [3,3]-sigmatropic rearrangement.[14] Nitrogen and carbon KIEs for the conversion of *N*-4-methoxyphenyl-*N*′-phenylhydrazine to the corresponding *p*-semidine and *o*-semidine were observed and the *p*-semidine rearrangement was assumed to be likely a concerted [1,5]-sigmatropic shift, whereas there was a slight 2,2′,6,6′-$^{13}C_4$ KIE for the *o*-semidine rearrangement.[15a–d] Accordingly, the π-complex theory was ruled out by Shine's kinetic experiments, but it has been revived by recent calculations.[16,17]

To date, the mechanisms for the formation of *p*-benzidines and *o*-benzidines in benzidine rearrangements have been verified clearly as [5,5]- and [3,3]-sigmatropic shifts, respectively. However, to the best of our knowledge, the formation of diphenylines, *p*-semidines, and *o*-semidines seem to undergo ambiguous pathways.[18] Further unraveling the mechanisms remain highly desirable in organic chemistry. After analyzing the structures of diphenylines, *p*-semidines, and *o*-semidines and considering the existence of the C[1,3] and O[1,3]-sigmatropic shifts, we propose that the N[1,3]-sigmatropic shift may be involved in the formation of diphenylines, *p*-semidines, and *o*-semidines in the benzidine rearrangement. Herein, we present our detailed experimental and computational studies on the N[1,3]-sigmatropic shift in the formation of semidines and diphenyline in the benzidine rearrangement. We believe that our in-depth mechanistic insight into the N[1,3]-sigmatropic shift in the benzidine rearrangement is critical not only to understand the benzidine rearrangement completely, but also to enrich the theory of heteroatom [1,3]-sigmatropic shifts.

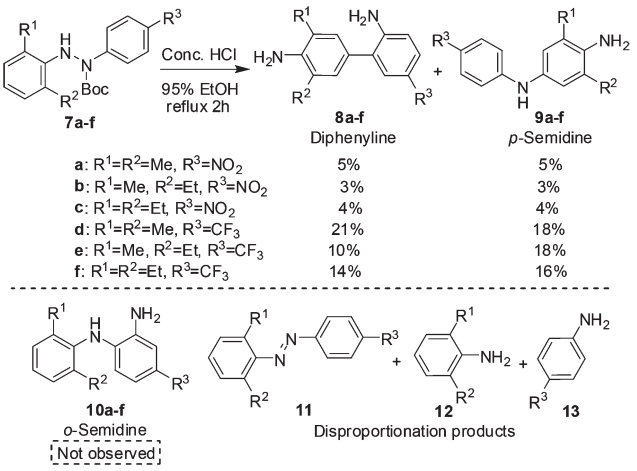

Scheme 2 Acid-catalyzed rearrangement of 2,4′,6-trisubstituted *N*,*N*′-diarylhydrazines **7**.

Results and discussion

Experimental investigation on the acid-catalyzed semidine and diphenyline rearrangements

Since the benzidine rearrangements can undergo a concerted [5,5]-sigmatropic rearrangement to produce *p*-benzidines as major products, or a [3,3]-sigmatropic shift to yield *o*-benzidines, we designed *N*,*N*′-diaryl hydrazines with 2,4′,6-substituents in order to prevent the formation of *p*-benzidine and *o*-benzidine products, simplifying the separation and determination of the rearrangement products. *N*,*N*′-Diaryl hydrazines **7** with different substituents were synthesized from 2,6-disubstituted *N*′-Boc-*N*-aryl hydrazines and 4-substituted aryl halides by a Cu(I)-catalyzed coupling reaction.[19]

We envisioned that the 2,4′,6-trisubstituted *N*,*N*′-diaryl hydrazines **7** would give rise to semidines and diphenylines (Scheme 2). *N*,*N*′-Diaryl hydrazine **7a** was first examined upon reflux in 95% ethanol for 2 h in the presence of concentrated HCl. After workup, we obtained the expected diphenyline **8a** in 5% yield and *p*-semidine **9a** in 5% yield, concomitant with the disproportionation products such as azobenzene **11a** and corresponding arylamines **12a** and **13a**. However, no *o*-semidine type product **10a** was observed. Other two nitro substituted *N*,*N*′-diaryl hydrazines **7b–c** gave similar results. With a trifluoromethyl substituent, *N*,*N*′-diaryl hydrazines **7d–f** underwent acid-catalyzed rearrangement to provide better results, affording 10–21% yields of the diphenylines **8d–f** and 16–18% yields of *p*-semidines **9d–f** with the corresponding disproportionation products (see ESI† for details). Moreover, all reactions were subjected to LC-MS analysis without the observation of the *o*-semidines **10**.

To obtain *o*-semidine type products, we designed 2,4,4′,6-tetrasubstituted *N*,*N*′-diaryl hydrazines **14**, which would suppress the formation of diphenyline and *p*-semidine products. Similarly, *N*,*N*′-diaryl hydrazines **14** were synthesized from 2,4,6-trisubstituted *N*′-Boc-*N*-aryl hydrazines and 4-substituted aryl halides *via* a Cu(I)-catalyzed coupling reaction. To our delight, the substrates **14a** and **14b** underwent acid-catalyzed rearrangement to provide the designed *o*-semidine type products **15a** and **15b** in 35% and 16% yields, respectively (Scheme 3), concomitant with the disproportionation products **13**, **16** and **17** (see ESI† for details).

Therefore, 2,4′,6-trisubstituted *N*,*N*′-diaryl hydrazines underwent acid-catalyzed rearrangement to produce diphenyline

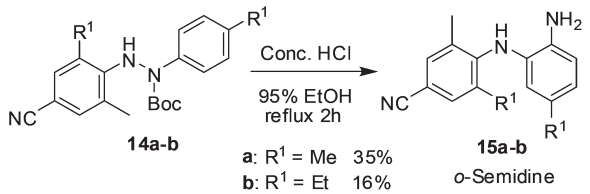

Scheme 3 Acid-catalyzed rearrangement of 2,4,4′,6-tetrasubstituted *N*,*N*′-diarylhydrazines **14**.

type products (up to 21% yield) and *p*-semidine type products (up to 18% yield), while 2,4,4′,6-tetrasubstituted *N*,*N*′-diaryl hydrazines gave rise to *o*-semidine type products (up to 35% yield). In all the acid-catalyzed rearrangements, competitive disproportionation reactions were inevitable.

Control experiments

It is unclear whether the formation of semidines and diphenylines are intramolecular or intermolecular processes, although it is well-known that the benzidine rearrangement is an intramolecular reaction for the formation of *o*- and *p*-benzidines.[20] We performed intercrossing experiments to clarify the mechanism (Scheme 4). A mixture of equimolar amounts of *N*,*N*′-diaryl hydrazines **14a** and **14b** was treated under the standard conditions. Only two *o*-semidines **15a** and **15b** were detected without the intercrossing *o*-semidines, as determined by LC-MS analysis (see ESI† for details). Likewise, the intercrossing experiment with equimolar amounts of the *N*,*N*′-diaryl hydrazines **7a** and **7e** was conducted and produced two diphenylines **8a** and **8e**, as well as two *p*-semidines **9a** and **9e** without any intercrossing products (see ESI† for details). The formation of no intercrossing products indicates that all the rearrangements are intramolecular processes.

To rule out a solvent-caged biradical mechanism for the rearrangements, radical trapping experiments were performed as well (Scheme 5). Treatment of hydrazine **7d** under the standard conditions with TEMPO gave rise to diphenyline **8d** in 22% yield and *p*-semidine **9d** in 17% yield. Hydrazine **14a** afforded *o*-semidine **15a** in 33% yield with TEMPO under the

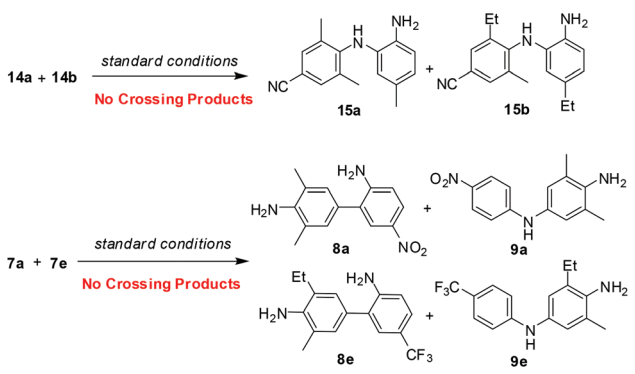

Scheme 4 Intercrossing experiments for the formation of *o*-semidines, *p*-semidines, and diphenylines.

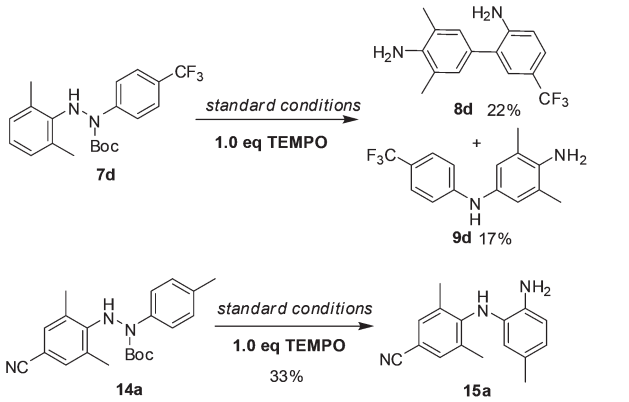

Scheme 5 Radical trapping experiments in the formation of *o*-semidine, *p*-semidine, and diphenyline type products.

standard conditions. The radical trapper has no significant effect on the conversion of the rearrangement, excluding a radical mechanism in a solvent cage. This is consistent with the radical-free process reported by Shine.[15] The results indicate that even if biradicals were generated, they formed disproportionation products rather than semidines and diphenylines.

Computational studies

DFT calculations[21] using the B3LYP/6-311++G(d,p) level were employed to locate all the stationary points involved.[22] Frequency calculations at the same level were performed to confirm each stationary point to be either an intermediate or a transition state structure. The free energies in solution were computed by a self-consistent reaction field (SCRF) using the conductor polarizable continuum model (CPCM) method in ethanol at the same level.[23]

***o*-Semidine rearrangement.** Our intercrossing and radical trapping experiments have excluded ionic and radical mechanisms. Thus, the formation of *o*-semidine products should be an intramolecular process for the acid-catalyzed benzidine rearrangement. We propose two possible intramolecular mechanisms for the *o*-semidine rearrangement: (1) a concerted N[1,3]-sigmatropic shift with a configuration inversion of the nitrogen atom, which is orbital symmetry allowed (Scheme 6, pathway A); (2) a tandem [3,3]- and C[1,3]-sigmatropic shifts process with a configuration inversion of the carbon atom (Scheme 6, pathway B).

To understand the above possible mechanisms, mono-protonated hydrazine **14a-H** as a representative model system was examined by DFT calculations (Fig. 2). Diprotonated hydrazine **14a-2H** was also taken into account, whereas the scission of the N–N bond took place spontaneously possibly due to the unstable vicinal dicationic structure. Another mono-protonated hydrazine **14a-H′** is more unstable than **14a-H** by 1.6 kcal mol^{-1} in terms of Gibbs free energy due to protonation on the weaker basic nitrogen atom. **14a-H** undergoes a concerted N[1,3]-sigmatropic shift through a transition state ***o*-TS1** with an activation free energy of 11.0 kcal mol^{-1} to afford a stable intermediate ***o*-Int1** (pathway A). In ***o*-TS1**, the

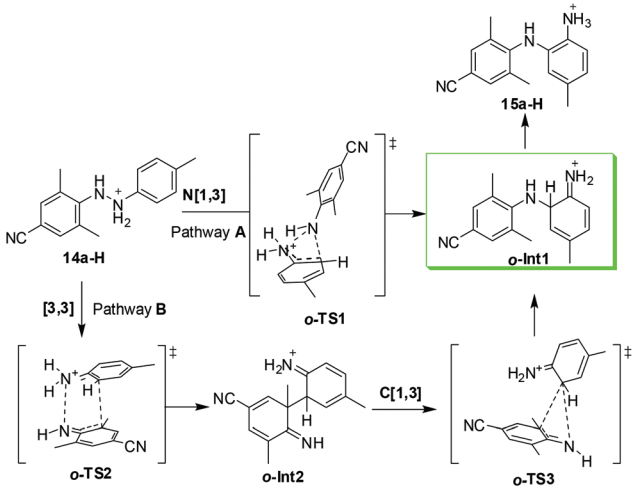

Scheme 6 Proposed mechanism of the *o*-semidine rearrangement.

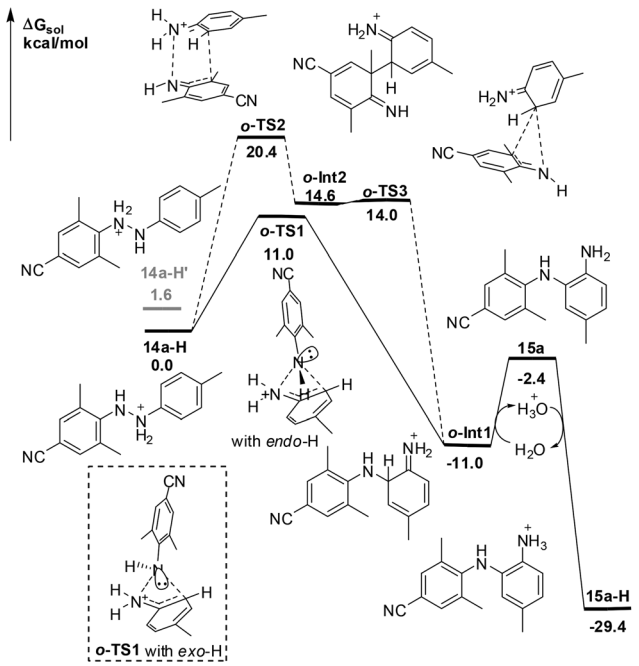

Fig. 2 Free energy profiles for the *o*-semidine rearrangement.

computed distances of the N–N bond breaking and the N–C bond making are 2.75 and 2.95 Å, respectively (Fig. 3). The alternative pathway B involves a [3,3]-sigmatropic shift *via* a transition state ***o*-TS2** with an activation free energy of 20.4 kcal mol^{-1}, leading to an intermediate ***o*-Int2**. The distances of the N–N bond cleavage and the C–C bond formation in ***o*-TS2** are 2.83 and 2.13 Å, respectively (Fig. 3). The following C[1,3]-sigmatropic shift *via* a transition state ***o*-TS3** is almost barrierless to form ***o*-Int1**. In the ***o*-TS3**, the computed C–C and C–N bonds in the four-membered ring transition state are almost dissociated due to the rigid ring. Finally, the assistance of a water molecule facilitates the tautomerization from the ***o*-Int1** to **15a-H**.

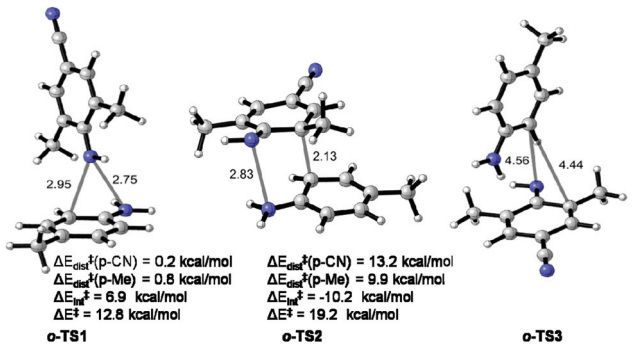

Fig. 3 Structures and distortion/interaction analysis of transition states for the *o*-semidine rearrangement. Distances of interest are reported in angstroms.

In addition, we attempted to calculate the potential profiles from **14a-H′** for the sake of comparison. However, unfortunately, its ***o*-TS1** cannot be located. On the other hand, the two stereoisomers of the ***o*-TS1** were also considered in the calculation (Fig. 2). On optimization, the potential energy of the ***o*-TS1** with *exo*-H decreased continuously till the ***o*-TS1** with *exo*-H was converted to the ***o*-TS1** with *endo*-H because the *endo*-H ***o*-TS1** shows less steric hindrance than the *exo*-H one. Additionally, a weak H–π interaction exists in *endo*-H ***o*-TS1** due to a distance between the H and the benzene ring of approximately 2.6 Å (see ESI† for details) and without the repelling interaction between the lone pair of electrons on the nitrogen and the π electron cloud of benzene ring (or called cyclohexadiene part). Both steric and electronic effects indicate that the transition state *endo*-H ***o*-TS1** is more stable than *exo*-H ***o*-TS1**. A similar phenomenon was observed in ***o*-TS3**. The results indicate that steric hindrance plays an important role in the stabilization of the *endo*-H transition states in both N and C[1,3] sigmatropic shifts.

Distortion/interaction analysis,[24] which is a powerful tool to understand the factors that stabilize the transition states, was employed to allow for deep understanding of the main reasons why ***o*-TS1** is lower in energy than ***o*-TS2** (Fig. 3). The activation energy ($\Delta E^{\ddagger}$) can be mainly separated into the distortion energy of anilines ($\Delta E^{\ddagger}_{\mathrm{dist}}$) and the interaction energy between the two distorted fragments ($\Delta E^{\ddagger}_{\mathrm{int}}$). In ***o*-TS1**, the interaction energy between the two fragments is very small, but both fragments are hardly distorted from initial equilibrium geometries. In contrast, there is much more distortion of the fragments in ***o*-TS2**, and this is only partially compensated for by more effective interaction. Thus, the pathway through ***o*-TS1** is favorable for the *o*-semidine rearrangement, which is dominantly attributed to low distortion in the transition state.

In terms of the *o*-semidine rearrangement, Shine and co-workers have reported KIE for the rearrangements of *N*-4-methoxyphenyl-*N*′-phenylhydrazine (**18**)[15a] and *N*,*N*′-di(4-chlorophenyl)hydrazine (**21**) (Scheme 7).[15b–e] The formation of *o*-semidine **19** from [^{15}N,^{15}N′]-**18** resulted in an average KIE of 1.074, while the generation of *o*-semidine **22** from [^{14}N,^{15}N′]-**21** and [2,2′,6,6′-^{13}C$_4$]-**21** furnished KIEs of 1.0155 and 0.9963,

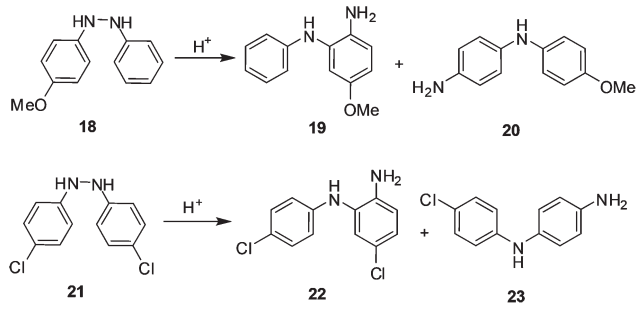

Scheme 7 Acid-catalyzed rearrangement of *N,N'*-diarylhydrazines **18** and **21**.

respectively. The ^{15}N KIE is more obvious than the ^{13}C KIE, and even an inverse ^{13}C kinetic isotope effect was observed close to unity. The KIE results indicate that the transition state in the rate-determining step should be an early (reactant-like) transition state rather than a late transition state, consistent with the calculated results because ***o*-TS1** in the N[1,3] sigmatropic shift is an early transition state, while ***o*-TS2** in the [3,3] sigmatropic shift is a late transition state. Thus, Shine's KIE results support the N[1,3]-sigmatropic shift mechanism for the formation of *o*-semidine.

Diphenyline and *p*-semidine rearrangements. For the diphenyline rearrangement, we put forward two possible intramolecular but stepwise pathways: tandem N[1,3]/[3,3]-sigmatropic shifts (pathway **C1**) and cascade [3,3]/C[1,3]-sigmatropic shifts (pathway **D1**). For the formation of *p*-semidines, we also propose two possible intramolecular but stepwise pathways: tandem N[1,3]/N[1,3]-sigmatropic shifts (pathway **C2**) and cascade [3,3]/[3,3]-sigmatropic shifts (pathway **D2**) (Scheme 8).

A representative model system with mono-protonated hydrazine **7a-H** was examined by DFT calculations to understand the proposed pathways (Fig. 4). **7a-H** could undergo the N[1,3]-sigmatropic shift *via* a transition state ***dp*-TS1** with an activation free energy of 17.0 kcal mol^{-1}. This step of the reaction is exergonic by 15.8 kcal mol^{-1}, giving a stable intermediate ***dp*-Int1** (pathway **C**). Once the intermediate ***dp*-Int1** is formed, two pathways can be followed: (i) the [3,3]-sigmatropic shift of ***dp*-Int1** *via* transition state ***d*-TS2** requires an activation energy of 31.5 kcal mol^{-1} (but only 15.7 kcal mol^{-1} in terms of the Gibbs free energy) to yield an unstable intermediate ***d*-Int2**, followed by tautomerization to deliver mono-protonated diphenyline **8a-H** (pathway **C1**); (ii) ***dp*-Int1** undergoes another N[1,3]-sigmatropic shift *via* a transition state ***p*-TS2**, requiring an activation energy of 36.3 kcal mol^{-1} (20.5 kcal mol^{-1} in terms of the Gibbs free energy) to give rise to a stable intermediate ***p*-Int2** (pathway **C2**). Alternatively, **7a-H** could also undergo a [3,3]-sigmatropic shift *via* transition state ***dp*-TS3** with an activation energy of 24.2 kcal mol^{-1} to yield an unstable intermediate ***dp*-Int3** (pathway **D**), which can further undergo two

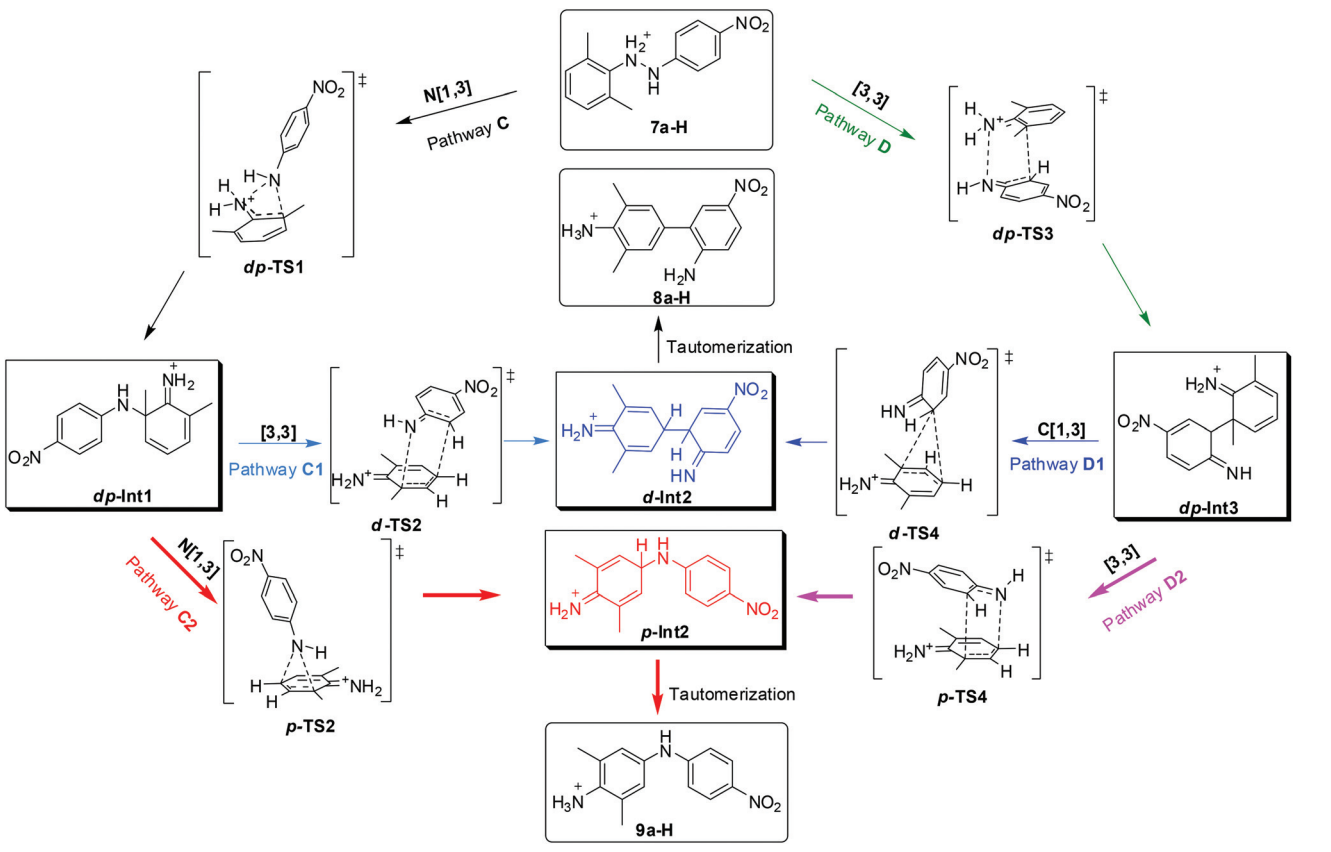

Scheme 8 Proposed mechanism for diphenyline and *p*-semidine rearrangements.

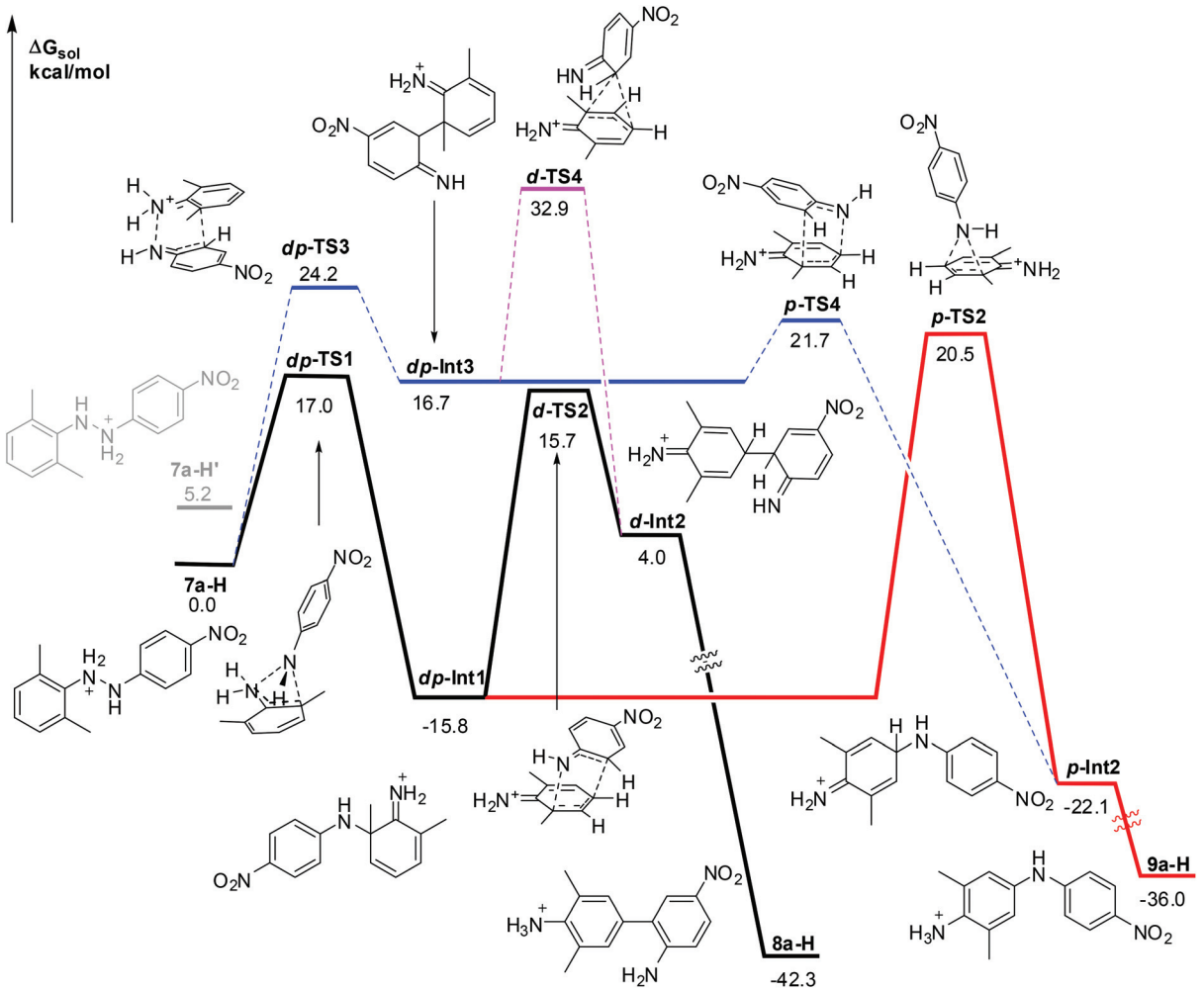

Fig. 4 Potential energy profiles of the diphenyline and *p*-semidine rearrangements.

different rearrangements: (i) the consequent C[1,3]-sigmatropic shift of ***dp*-Int3** through ***d*-TS4** requires 32.9 kcal mol^{-1} in terms of the Gibbs free energy (the activation energy of 16.2 kcal mol^{-1}), leading to **8a-H** (pathway **D1**); (ii) the [3,3]-sigmatropic shift of ***dp*-Int3** results in the formation of **9a-H** with an activation energy of 5.0 kcal mol^{-1} (21.7 kcal mol^{-1} in terms of the Gibbs free energy) (pathway **D2**).

Therefore, pathway **C** is favored over pathway **D** by 7.2 kcal mol^{-1} in the first step of the tandem processes and predominant in each of the second steps in terms of the Gibbs free energy. Although the two second steps in pathway D could occur with relative lower activation energies (16.2 kcal mol^{-1} and 5.0 kcal mol^{-1}, respectively) than those in pathway C, it is very difficult for the first step reaction in pathway D due to its higher activation energy (24.2 kcal mol^{-1}) and endergonic process. However, the intermediate ***dp*-Int1** is more stable than ***dp*-Int3** by 32.5 kcal mol^{-1}. In the consequent step from ***dp*-Int1**, two different pathways can correspond to mono-protonated diphenyline **8a-H** (pathway **C1**) and mono-protonated *p*-semidine **9a-H** (pathway **C2**). Eventually, our calculated results draw the conclusion that the first N[1,3] shift is the rate-limiting step for the formation of diphenyline **8a**, while the second N[1,3] shift is both the rate-limiting and the rate-determining step for the generation of *p*-semidine **9a**. The computed distances of all transition states are in a reasonable range except for those of ***d*-TS4** which reach the extent of scission (Fig. 5).

Shine and co-workers have reported the KIEs for the rearrangement of *N*,*N*′-diphenylhydrazine (**1**) into diphenyline (**3**).[13e,14d] The KIEs for [^{15}N,^{15}N′]-**1** and [2,2′,6,6′-^{13}C$_4$]-**1** are 1.0367 and 0.9953, respectively. For [4,4′-^{13}C$_2$]-**1**, no carbon KIE was observed. These findings imply that the cleavage of the N–N bond and the formation of the N–C2 bond are in the rate-limiting step. Similarly, a more obvious ^{15}N KIE (variation magnitude) was observed than ^{13}C KIE, an inverse ^{13}C KIE. The KIE results reveal that the transition state in the rate-limiting step should be an early (reactant-like) transition state rather than a late transition state, consistent with our calculated tandem N[1,3]/[3,3] sigmatropic shift mechanism with the first N[1,3] sigmatropic shift as the rate-limiting step because the ***dp*-TS1** in the first N[1,3] sigmatropic shift is an early transition state with a higher potential energy of

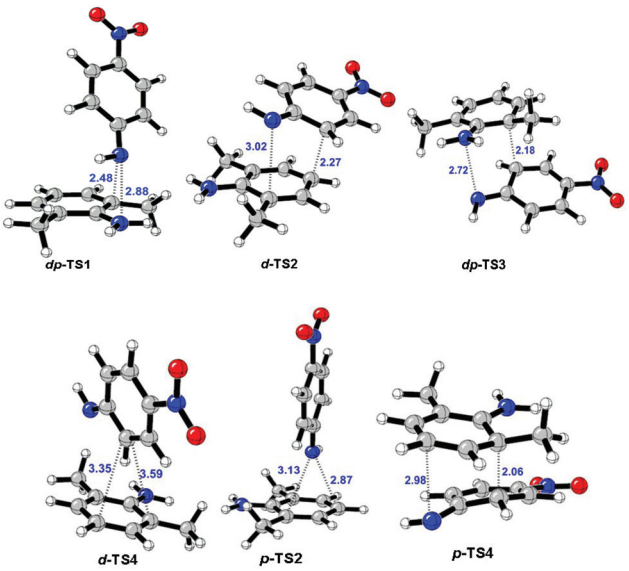

Fig. 5 Structures of transition states for the *p*-semidine and diphenyline rearrangements. Distances of interest are reported in angstroms.

17.0 kcal mol^{-1}, while the ***d*-TS2** in the second [3,3] sigmatropic shift is a late transition state. On the other hand, the transition state ***dp*-TS3** is a late transition state and locates at a higher potential energy of 24.2 cal mol^{-1} as well. However ***d*-TS4** is also an early transition state, but with the highest potential energy of 32.9 cal mol^{-1}. After this analysis, we can conclude that our proposed tandem N[1,3]/[3,3]-sigmatropic shifts and the first N[1,3] sigmatropic shift as the rate-limiting step for the formation mechanism of the diphenylines are consistent with Shine's KIE observation.

The averaged KIEs for the formation of *p*-semidine **20** from [^{15}N,^{15}N′]-**18** and [4′-^{14}C]-**18** were measured as 1.0296 and 1.039, respectively.[15a,e] On the basis of the KIE results, a concerted [1,5]-sigmatropic shift through a six-membered ring transition state from the protonated **18** was proposed by Shine. However, the proposed transition state for the concerted [1,5]-sigmatropic shift seems to have a large distorted energy with the rigid benzene ring. It is not a reasonable process. However, the KIEs support our tandem N[1,3]/N[1,3] sigmatropic shift process with the second one as the rate-limiting step.

In addition, the formation of *p*-semidine **23** from [^{15}N,^{15}N′]-**21**, [^{14}N,^{15}N′]-**21**, [4,4′-$^{13}C_2$]-**21**, [4-^{14}C]-**21**, and [2,2′,6,6′-$^{13}C_4$]-**21** furnished KIEs of 1.0282, 1.0162, 0.9934, 1.0029, and 0.9973, respectively.[15b–e] The results indicate that the rate-limiting step involves the nitrogen atom, *ortho* and *para* carbon atoms, and also matched with our proposed tandem N[1,3]/N[1,3]-sigmatropic shift mechanism with the second N[1,3]-sigmatropic shift as the rate-limiting step for the formation of *p*-semidine. From a viewpoint of energy, it is reasonable to consider the formation mechanism of *p*-semidines as a tandem N[1,3]/N[1,3]-sigmatropic shift mechanism with the second N[1,3]-sigmatropic shift as the rate-limiting step. However, the carbon KIEs for both *ortho* and *para* carbon atoms are very small, unlike the transition states ***o*-TS1** and ***dp*-TS1**, no obvious relationship between their variation magnitudes and the transition state structure of ***p*-TS2** is observed due to the experimental determination precision. The small carbon KIEs can possibly be attributed to the rigid benzene ring involved in the transition state ***p*-TS2**. Small carbon KIEs were observed in several cyclic transition states previously.[25–27]

In the rearrangements of diphenylines, *o*- and *p*-semidines, the inverse carbon KIE is generally observed. Unlike deuterium KIE, the heavy atom primary inverse KIEs have seldom been observed previously.[28] They were assumed to generate due to nonlinearity in the transition states, causing bending modes in addition to stretching modes in vibrations. In our investigated rearrangements, all the transition states in the rate-limiting steps are four-membered ring ones. Thus, the inverse carbon KIE can be attributed to the nonlinear transition states in the rate-limiting steps.

Influence of substituents on transition states and KIEs. The substituents can change the transition states (early or late transition states), resulting in KIE changes, even normal to inverse or inverse to normal.[28] Our investigated *N*,*N*′-diarylhydrazines are different from those in the KIE experiments. To verify the impact of the substituents on the phenyl group(s) on the transition states in the semidine and diphenyline rearrangements, we further calculated the potential energy profiles for the formation of semidines and diphenylines from *N*,*N*′-diarylhydrazines **1**, **18**, and **21** (Table 1). The results indicated that all the transition states ***o*-TS1** for *N*,*N*′-diarylhydrazines **14a**, **1**, **18**, and **21** are early transition states (Table 1, columns 1 and 2), indicating that these diarylhydrazines should show similar ^{15}N and ^{13}C KIEs in their *o*-semidine rearrangements. That is, the reported KIEs of **18** and **21** can represent those in our studied system of *N*,*N*′-diarylhydrazine **14a**.

For *p*-semidine rearrangements, except for *N*,*N*′-diphenylhydrazine **1**, for which ***p*-TS2** cannot be located in its calculation

Table 1 The calculated energies of transition states and intermediates in the formation of diphenylines and semidines from different diarylhydrazines in pathways A and C (ΔG and $\Delta G^{\neq}$ in kcal mol^{-1})

Hydrazine	$\Delta G^{\neq}$ (*o*-**TS1**)	ΔG (*o*-**Int1**)	$\Delta G^{\neq}$ (*dp*-**TS1**)	ΔG (*dp*-**Int1**)	$\Delta G^{\neq}$ (*d*-**TS2**)	ΔG (*d*-**Int2**)	$\Delta G^{\neq}$ (*p*-**TS2**)	ΔG (*p*-**Int2**)
14a	11.0	−11.0	—	—	—	—	—	—
7a	—	—	17.0	−15.0	15.7	4.0	20.5	−22.1
1	14.7	−13.0	14.7	−13.0	15.0	4.7	NL	NC
18	14.2	−8.9	14.8	1.7	NL	NC	16.4	−12.4
21	12.8	−10.8	12.8	−10.8	NL	NC	13.3	−19.1

NL = not located. NC = not calculated.

(consistent with trace *p*-semidine **5** generated in the experiment), the transition states ***p*-TS2** for both *N*,*N*′-diarylhydrazines **18** and **21** show higher potential energy than the corresponding ***dp*-TS1** and are early transition states, indicating that the second N[1,3] sigmatropic shift is the rate-limiting step in the formation of the corresponding *p*-semidines **20** and **23** as in the formation of *p*-semidine **9a**. The hydrazine **21** shows a similar potential energy profile to that of the hydrazine **7a** in the *p*-semidine rearrangement. Thus, the KIEs of **21** should represent those of **7a**. However, the hydrazine **21** possesses lower energy barriers than **7a** in both N[1,3] sigmatropic shifts. This is the reason why **7a** yields **9a** in a low yield of 5%, while **21** generated **23** in a relatively high yield of 12%.

Considering the diphenyline rearrangements, transition states ***d*-TS2** are not located in the calculation for hydrazines **18** and **21**, in agreement with no observation of the corresponding diphenylines experimentally. Thus, only *N*,*N*′-diphenylhydrazine **1** was compared with hydrazine **7a**. However, unexpected results were obtained. For hydrazine **7a**, its transition state ***d*-TS2** is slightly higher (0.3 kcal mol^{-1}) than its ***dp*-TS1** in terms of the Gibbs free energy, but a less obvious difference is seen from the viewpoint of calculation. Importantly, the ***dp*-TS1** of hydrazine **1** is an early transition state as in hydrazine **7a**. It is matched with the variation magnitudes of its ^{15}N and ^{13}C KIEs. The KIEs of hydrazine **1** could reflect a feature of the diphenyline rearrangements. Although it is difficult to provide an undoubted mechanism for the formation of diphenylines in the benzidine rearrangement on the basis of the current information, our proposed mechanism is a more reasonable one than proposed until now and our current investigation provides a further new insight and comprehensive understanding on the *o*- and *p*-semidine and diphenyline rearrangements.

Conclusion

In summary, to search for the existence of the N[1,3]-sigmatropic shift and to further elucidate the formation mechanisms of *o*/*p*-semidines and diphenylines, we have investigated the mechanisms of the acid-catalyzed semidines and diphenyline rearrangements with designed *N*,*N*′-diarylhydrazines. After a systematic investigation of experiments and theoretical calculations, it is reasonable to consider the acid-catalyzed *o*-semidine rearrangement as a N[1,3]-sigmatropic shift, *p*-semidine rearrangement as tandem N[1,3]/N[1,3]-sigmatropic shifts, and diphenyline rearrangement as cascade N[1,3]/[3,3]-sigmatropic shifts. The N[1,3]-sigmatropic shift is orbital suprafacial symmetry allowed with an inversion of the migrating nitrogen atom. The proposed intramolecular processes are supported by intercrossing experiments, radical trapping experiments, and KIE observations measured by Shine. The current results not only provide a comprehensive understanding of the formation of *o*/*p*-semidines and diphenylines in the benzidine rearrangement, but also disclose a novel N[1,3]-sigmatropic shift that has potential mechanistic possibility in other reactions.

Experimental section

General information

Melting points were obtained on a melting point apparatus and are uncorrected. ^1H NMR and ^{13}C NMR spectra were recorded on a 300 MHz or 400 MHz spectrometer with TMS as an internal standard in $CDCl_3$ solution. IR spectra were taken on a FT-IR spectrometer in KBr. HRMS data were obtained with an LC/MSD TOF mass spectrometer. Purification of reaction products was carried out by column chromatography using silica gel (200–300 mesh). TLC separations were performed on silica gel G plates with petroleum ether–ethyl acetate, and the plates were visualized with UV light.

General procedure for the synthesis of *N*-Boc-*N*,*N*′-diaryl hydrazines 7 and 14

A round bottom flask was charged with *N*′-Boc-*N*-aryl hydrazine (**24**, 48 mmol), 4-substituted iodobenzene (40 mmol), CuI (0.78 g, 4 mmol), 1,10-phenanthroline (1.44 g, 8 mmol), Cs_2CO_3 (15.64 g, 48 mmol) and 40 mL of dry DMF at room temperature. The reaction mixture was degassed, charged with N_2 gas and heated to 80 °C. After 4–5 h, the resulting mixture was cooled to room temperature, diluted with ethyl acetate (100 mL), and filtered. The filtrate was then washed twice with brine (2 × 100 mL). The organic layer was dried over anhydrous magnesium sulfate, filtered, and concentrated under reduced pressure. The residue was purified by flash chromatography with a mixture of petroleum ether and ethyl acetate as an eluent to afford the desired product, which was recrystallized from a mixture of petroleum ether and ethyl acetate to give crystals **7** or **14**.

***tert*-Butyl 2-(2,6-dimethylphenyl)-1-(4-nitrophenyl)hydrazinecarboxylate (7a).** Orange crystals, 2.57 g, yield 18%, m.p. 153–154 °C, ^1H NMR (300 MHz, $CDCl_3$) δ: 1.27 (s, 9 H), 2.17 (s, 6 H), 6.27 (s, 1H), 6.82 (t, J = 7.4 Hz, 1 H), 6.97 (d, J = 7.4 Hz, 2 H), 8.07–8.12 (m, 2 H), 8.19–8.25 (m, 2 H). ^{13}C NMR (75 MHz, $CDCl_3$) δ: 153.3, 149.3, 143.3, 142.8, 129.7, 124.8, 124.1, 121.9, 119.7, 83.7, 27.6, 19.0. IR (KBr) ν (cm^{-1}): 3359, 2978, 2932, 1721, 1590, 1514, 1476, 1308. HRMS (ESI) calcd for $C_{19}H_{23}N_3O_4$ $[M + H]^+$ m/z: 358.1761, found 358.1769.

***tert*-Butyl 2-(2-ethyl-6-methylphenyl)-1-(4-nitrophenyl)hydrazinecarboxylate (7b).** Orange crystals, 2.38 g, yield 16%, m.p. 118–119 °C, ^1H NMR (300 MHz, $CDCl_3$) δ: 1.19 (t, J = 7.5 Hz, 3 H), 1.26 (s, 9 H), 2.15 (s, 3 H), 2.56 (q, J = 7.5 Hz, 2 H), 6.34 (s, 1H), 6.85–7.03 (m, 3 H), 8.06–8.12 (m, 2 H), 8.20–8.25 (m, 2 H). ^{13}C NMR (50 MHz, $CDCl_3$) δ: 153.4, 149.4, 143.0, 142.8, 131.2, 129.8, 127.3, 125.3, 124.1, 122.1, 119.8, 83.7, 27.6, 24.7, 19.5, 14.2. IR (KBr) ν (cm^{-1}): 3359, 2974, 2932, 2875, 1716, 1590, 1515, 1469, 1342, 1113. HRMS (ESI) calcd for $C_{20}H_{25}N_3O_4$ $[M + H]^+$ m/z: 372.1918, found 372.1914.

***tert*-Butyl 2-(2,6-diethylphenyl)-1-(4-nitrophenyl)hydrazinecarboxylate (7c).** Orange crystals, 2.00 g, yield 13%, m.p. 164–165 °C, ^1H NMR (300 MHz, $CDCl_3$) δ: 1.15 (t, J = 7.5 Hz, 6 H), 1.26 (s, 9 H), 2.52 (q, J = 7.5 Hz, 4 H), 6.37 (s, 1 H), 6.94–7.04 (m, 3 H), 8.07–8.12 (m, 2 H), 8.21–8.26 (m, 2 H). ^{13}C NMR (50 MHz, $CDCl_3$) δ: 153.5, 149.4, 143.2,

142.3, 131.9, 127.3, 124.1, 122.6, 120.1, 83.8, 27.7, 24.9, 14.4. IR (KBr) ν (cm^{-1}): 3349, 2983, 1721, 1589, 1492, 1441, 1339. HRMS (ESI) calcd for $C_{21}H_{27}N_3O_4$ $[M + H]^+$ *m*/*z*: 386.2074, found 386.2089.

***tert*-Butyl 2-(2,6-dimethylphenyl)-1-(4-(trifluoromethyl)phenyl)-hydrazinecarboxylate (7d).** Colorless crystals, 5.63 g, yield 37%, m.p. 105–106 °C, ^{1}H NMR (300 MHz, $CDCl_3$) δ: 1.28 (s, 9 H), 2.19 (s, 6 H), 6.23 (s, 1 H), 6.80 (t, J = 7.5 Hz, 1 H), 6.95 (d, J = 7.5 Hz, 2 H), 7.59 (d, J = 8.7 Hz, 2 H), 7.95 (d, J = 8.7 Hz, 2 H). ^{13}C NMR (50 MHz, $CDCl_3$) δ: 153.8, 146.7, 143.6, 129.6, 125.3 (q, J_1 = 3.8 Hz), 125.2 (q, J_2 = 32.5 Hz), 125.0, 124.3 (q, J_3 = 270 Hz), 121.6, 120.4, 82.8, 27.6, 18.9. IR (KBr) ν (cm^{-1}): 3340, 2982, 1697, 1618, 1525, 1474, 1323. HRMS (ESI) calcd for $C_{20}H_{23}F_3N_2O_2$ $[M + H]^+$ *m*/*z*: 381.1784, found 381.1799.

***tert*-Butyl 2-(2-ethyl-6-methylphenyl)-1-(4-(trifluoromethyl)-phenyl)hydrazinecarboxylate (7e).** Colorless crystals, 7.10 g, yield 45%, m.p. 121–121.5 °C, ^{1}H NMR (300 MHz, $CDCl_3$) δ: 1.18 (t, J = 7.5 Hz, 3 H), 1.28 (s, 9 H), 2.17 (s, 3 H), 2.56 (q, J = 7.5 Hz, 2 H), 6.30 (s, 1H), 6.84–7.02 (m, 3 H), 7.58–7.61 (m, 2 H), 7.93–7.96 (m, 2 H). ^{13}C NMR (50 MHz, $CDCl_3$) δ: 153.9, 146.6, 143.0, 131.4, 129.7, 127.2, 125.5, 125.5 (q, J_2 = 32.5 Hz), 125.4 (q, J_3 = 3.7 Hz), 124.3 (q, J_1 = 270 Hz), 122.0, 120.7, 83.0, 27.7, 24.7, 19.5, 14.3. IR (KBr) ν (cm^{-1}): 3367, 2975, 2932, 2869, 1720, 1615, 1469, 1322, 1160, 1115. HRMS (ESI) calcd for $C_{21}H_{25}F_3N_2O_2$ $[M + H]^+$ *m*/*z*: 395.1941, found 395.1937.

***tert*-Butyl 2-(2,6-diethylphenyl)-1-(4-(trifluoromethyl)phenyl)-hydrazinecarboxylate (7f).** Colorless crystals, 4.41 g, yield 27%, m.p. 83–84 °C, ^{1}H NMR (300 MHz, $CDCl_3$) δ: 1.15 (t, J = 7.5 Hz, 6 H), 1.27 (s, 9 H), 2.54 (q, J = 7.5 Hz, 4 H), 6.34 (s, 1H), 6.90–7.03 (m, 3 H), 7.58–7.61 (m, 2 H), 7.92–7.95 (m, 2 H). ^{13}C NMR (50 MHz, $CDCl_3$) δ: 154.1, 146.7, 142.5, 132.1, 127.3, 125.7 (q, J_2 = 32.3 Hz), 125.4 (q, J_3 = 3.7 Hz), 124.3 (q, J_1 = 270 Hz), 122.4, 120.9, 83.0, 27.8, 24.9, 14.5. IR (KBr) ν (cm^{-1}): 3365, 2971, 2935, 2876, 1720, 1615, 1456, 1322, 1160, 1123. HRMS (ESI) calcd for $C_{22}H_{27}F_3N_2O_2$ $[M + H]^+$ *m*/*z*: 409.2097, found 409.2086.

***tert*-Butyl 2-(4-cyano-2,6-dimethylphenyl)-1-(*p*-tolyl)hydrazinecarboxylate (14a).** Colorless crystals, 4.50 g, yield 32%, m.p. 157–159 °C, ^{1}H NMR (300 MHz, $CDCl_3$) δ: 1.33 (s, 9 H), 2.23 (s, 6 H), 2.32 (s, 3 H), 6.43 (s, 1 H), 7.14 (m, 2 H), 7.21 (s, 2 H), 7.47 (m, 2 H). ^{13}C NMR (75 MHz, $CDCl_3$) δ: 154.1, 148.0, 140.4, 134.3, 133.2, 128.9, 125.6, 121.6, 119.6, 103.7, 82.5, 27.9, 20.7, 19.0. IR (KBr) ν (cm^{-1}): 3356, 2977, 2926, 2218, 1717. HRMS (ESI) calcd for $C_{21}H_{25}N_3O_2$ $[M + H]^+$ *m*/*z*: 352.2020, found 352.2031.

***tert*-Butyl 2-(4-cyano-2-ethyl-6-methylphenyl)-1-(4-ethylphenyl)-hydrazinecarboxylate (14b).** Colorless crystals, 5.62 g, yield 37%, m.p. 164–164.5 °C, ^{1}H NMR (300 MHz, $CDCl_3$) δ: 1.20 (t, J = 7.5 Hz, 3 H), 1.23 (t, J = 7.5 Hz, 3 H), 1.33 (s, 9 H), 2.24 (s, 3 H), 2.59 (q, J = 7.5 Hz, 2 H), 2.64 (q, J = 7.5 Hz, 2 H), 6.45 (d, J = 4.1 Hz, 1 H), 7.17 (m, 2 H), 7.23 (s, 1 H), 7.28 (s, 1 H), 7.49 (m, 2 H). ^{13}C NMR (75 MHz, $CDCl_3$) δ: 154.1, 147.6, 140.5, 140.5, 133.1, 131.5, 130.8, 127.6, 126.0, 121.6, 119.7, 103.8, 82.3, 28.0, 27.8, 24.3, 19.4, 15.3, 13.6, 8.7. IR (KBr) ν (cm^{-1}): 3343, 2964, 2929, 2219, 1718. HRMS (ESI) calcd for $C_{23}H_{29}N_3O_2$ $[M + H]^+$ *m*/*z*: 380.2333, found 380.2346.

General procedure for the acid-catalyzed rearrangements of *N*,*N*′-diaryl hydrazines 7 and 14

A round bottom flask was charged with *N*,*N*′-diaryl hydrazine (**7** or **14**, 1 mmol), 95% ethanol (10 mL), and conc. HCl (0.5 mL) under nitrogen at room temperature. The reaction mixture was refluxed for 2 h, then cooled to room temperature, neutralized with solid $NaHCO_3$, filtered, and concentrated. The residue was purified by flash column chromatography.

3′,5′-Dimethyl-5-nitro-1,1′-biphenyl-2,4′-diamine (8a). Yellowish crystals, 13 mg, yield 5%, m.p. 186–188 °C, ^{1}H NMR (300 MHz, $CDCl_3$) δ: 2.23 (s, 6 H), 3.73 (s, 2 H), 4.54 (s, 2 H), 6.67 (q, J_1 = 2.6 Hz, 1 H), 7.01 (s, 2 H), 8.01 (dd, J_1 = 2.6 Hz, J_2 = 2.3 Hz, 2 H). ^{13}C NMR (126 MHz, $CDCl_3$) δ: 150.1, 142.9, 139.2, 128.6, 127.1, 126.7, 126.2, 124.5, 122.3, 113.6, 17.7. IR (KBr) ν (cm^{-1}): 3433, 3340, 2962, 2873, 1284. HRMS (ESI) calcd for $C_{14}H_{15}N_3O_2$ $[M + H]^+$ *m*/*z*: 258.1237, found 258.1245.

3′-Ethyl-5′-methyl-5-nitro-1,1′-biphenyl-2,4′-diamine (8b). Brown crystals, 8 mg, yield 3%, m.p. 131–133 °C, ^{1}H NMR (300 MHz, $CDCl_3$) δ: 1.29 (t, J_1 = 7.5 Hz, 3 H), 2.34 (s, 3 H), 2.58 (q, J_1 = 7.5 Hz, 2 H), 3.77 (s, 2 H), 4.55 (s, 2 H), 6.68 (dt, J_2 = 1.6 Hz, J_3 = 2.7 Hz, 1 H), 7.02 (s, 2 H), 8.00 (d, J_3 = 2.7 Hz, 1 H), 8.03 (d, J_2 = 1.6 Hz, 2 H). ^{13}C NMR (126 MHz, $CDCl_3$) δ: 150.3, 142.3, 138.9, 128.4, 128.0, 127.1, 126.7, 126.5, 126.2, 124.4, 122.5, 113.5, 24.2, 17.7, 12.9. IR (KBr) ν (cm^{-1}): 3482, 3376, 2966, 2873, 1307. HRMS (ESI) calcd for $C_{15}H_{17}N_3O_2$ $[M + H]^+$ *m*/*z*: 272.1394, found 272.1410.

***N*,*N*′-(3′,5′-Diethyl-5-nitro-1,1′-biphenyl-2,4′-diyl)diacetamide (8c).** A mixture (48 mg) of diphenyline and *p*-nitroaniline in 5 mL of $(Ac)_2O$ was stirred at room temperature for 12 h. The resulting mixture was diluted with water (50 mL), and extracted with ethyl acetate (2 × 50 mL). The organic layer was washed with saturated $NaHCO_3$ (50 mL), brine (50 mL), dried over anhydrous Na_2SO_4, filtered, concentrated under reduced pressure and purified by flash chromatography with a mixture of petroleum ether and ethyl acetate as an eluent to afford **8c**. Yellowish solid, 15 mg, yield 4%, m.p. 230–232 °C, ^{1}H NMR (300 MHz, DMSO-d_6) δ: 1.17 (t, J_1 = 7.5 Hz, 6 H), 2.03 (s, 3 H), 2.10 (s, 3 H), 2.59 (q, J_1 = 7.5 Hz, 4 H), 7.23 (s, 2 H), 7.99 (d, J_3 = 8.9 Hz, 1H), 8.12 (d, J_2 = 2.6 Hz, 1H), 8.22 (dd, J_2 = 2.6 Hz, J_3 = 8.9 Hz, 1H), 9.34 (s, 1 H), 9.68 (s, 1 H). ^{13}C NMR (126 MHz, DMSO-d_6) δ: 169.1, 168.8, 143.9, 142.0, 141.3, 135.2, 135.1, 134.5, 126.4, 126.0, 125.3, 122.8, 24.4, 23.4, 22.6, 14.8. IR (KBr) ν (cm^{-1}): 3250, 3246, 2962, 2928, 2866, 2847, 1654, 1508, 1350, 1274. HRMS (ESI) calcd for $C_{20}H_{23}N_3O_4$ $[M + H]^+$ *m*/*z*: 370.1761, found 370.1768.

3′,5′-Dimethyl-5-trifluoromethyl-1,1′-biphenyl-2,4′-diamine (8d). Colorless crystals, 59 mg, yield 21%, m.p. 74–75 °C, ^{1}H NMR (300 MHz, $CDCl_3$) δ: 2.23 (s, 6 H), 3.70 (brs, 2 H), 4.06 (brs, 2 H), 6.73 (d, J = 9.0 Hz, 1 H), 7.02 (s, 2 H), 7.32 (m, 2 H). ^{13}C NMR (126 MHz, $CDCl_3$) δ: 146.8, 142.4, 128.6, 127.5, 127.5 (q, J = 3.6 Hz), 127.3, 124.9 (q, J = 270.6 Hz), 124.7 (q, J = 3.6 Hz), 122.11, 120.0 (q, J = 32.4 Hz), 114.4, 17.6. IR (KBr) ν (cm^{-1}): 3481, 3386, 2933, 2857, 1108. HRMS (ESI) calcd for $C_{15}H_{15}F_3N_2$ $[M + H]^+$ *m*/*z*: 281.1260, found 281.1276.

3′-Ethyl-5′-methyl-5-trifluoromethyl-1,1′-biphenyl-2,4′-diamine (8e). Yellowish oil, 29 mg, yield 10%, ^{1}H NMR (300 MHz,

$CDCl_3$) δ: 1.28 (t, J_1 = 7.5 Hz, 3 H), 2.23 (s, 3 H), 2.58 (q, J_1 = 7.5 Hz, 2 H), 3.72 (brs, 2 H), 4.08 (s, 2 H), 6.75 (d, J_2 = 8.4 Hz, 1 H), 7.03 (s, 2 H), 7.33 (d, J_2 = 8.4 Hz, 1H), 7.34 (s, 1H). ^{13}C NMR (126 MHz, $CDCl_3$) δ: 146.8, 141.8, 128.4, 127.8, 127.6, 127.4 (q, J = 3.6 Hz), 127.4, 126.5, 124.9 (d, J = 270.7 Hz), 124.7 (q, J = 3.7 Hz), 122.3, 119.8 (q, J = 32.3 Hz), 114.4, 24.2, 17.6, 12.9. IR (KBr) ν (cm^{-1}): 3481, 3386, 2966, 2873, 1108. HRMS (ESI) calcd for $C_{16}H_{17}F_3N_2$ $[M + H]^+$ m/z: 295.1417, found 295.1414.

3′,5′-Diethyl-5-trifluoromethyl-1,1′-biphenyl-2,4′-diamine (8f). Yellowish oil, 43 mg, yield 14%, ^{1}H NMR (300 MHz, $CDCl_3$) δ: 1.29 (t, J_1 = 7.5 Hz, 6 H), 2.58 (q, J_1 = 7.5 Hz, 4 H), 3.77 (brs, 2 H), 4.09 (brs, 2 H), 6.75 (d, J_2 = 8.1 Hz, 1 H), 7.04 (s, 2 H), 7.33 (d, J_2 = 8.1 Hz, 1 H), 7.35 (s, 1 H). ^{13}C NMR (126 MHz, $CDCl_3$) δ 146.8, 141.3, 128.1, 127.8, 127.6, 127.5 (q, J = 3.7 Hz), 126.4, 124.9 (q, J = 270.7 Hz), 124.8 (q, J = 3.7 Hz), 120.0 (q, J = 32.4 Hz), 114.5, 24.3, 13.0. IR (KBr) ν (cm^{-1}): 3483, 3389, 2966, 2874, 1108. HRMS (ESI) calcd for $C_{17}H_{19}F_3N_2$ $[M + H]^+$ m/z: 309.1573, found 309.1577.

3,5-Dimethyl-N^1-(4-nitrophenyl)benzene-1,4-diamine (9a). Orange crystals, 13 mg, yield 5%, m.p. 193–195 °C, ^{1}H NMR (300 MHz, $CDCl_3$) δ: 2.20 (s, 6 H), 3.63 (s, 2 H), 6.04 (s, 1 H), 6.71 (d, J = 9.2 Hz, 2 H), 6.83 (s, 2 H), 8.07 (d, J = 9.2 Hz, 2 H). ^{13}C NMR (126 MHz, $CDCl_3$) δ: 152.4, 141.0, 138.6, 129.0, 126.4, 124.8, 122.8, 112.3, 17.7. IR (KBr) ν (cm^{-1}): 3363, 2962, 1301. HRMS (ESI) calcd for $C_{14}H_{15}N_3O_2$ $[M + H]^+$ m/z: 258.1237, found 258.1249.

***N*-(2-Ethyl-6-methyl-4-((4-nitrophenyl)amino)phenyl)acetamide (9b).** A mixture (36 mg) of *p*-semidine and *p*-nitroaniline in 5 mL of $(Ac)_2O$ was stirred at room temperature for 12 h. The resulting mixture was diluted with water (50 mL), and extracted with ethyl acetate (2 × 50 mL). The organic layer was washed with saturated $NaHCO_3$ (50 mL), brine (50 mL), dried over anhydrous Na_2SO_4, filtered, concentrated under reduced pressure and purified by flash chromatography with a mixture of petroleum ether and ethyl acetate as an eluent to afford **9b**. Yellow solid, 9 mg, yield 3%, m.p. 256–259 °C, ^{1}H NMR (300 MHz, DMSO-d_6) δ: 1.10 (t, J = 7.5 Hz, 3 H), 2.04 (s, 3 H), 2.12 (s, 3 H), 2.52 (q, J = 7.5 Hz, 2 H), 6.93 (s, 1 H), 6.96 (s, 1 H), 7.04 (m, 2 H), 8.08 (m, 2 H), 9.14 (s, 1 H), 9.22 (s, 1 H). ^{13}C NMR (126 MHz, DMSO-d_6) δ: 168.5, 151.0, 142.3, 138.2, 137.7, 136.9, 130.5, 126.2, 120.0, 118.5, 113.2, 24.4, 22.5, 18.2, 14.4. IR (KBr) ν (cm^{-1}): 3445, 2961, 2920, 1654, 1581, 1312. HRMS (ESI) calcd for $C_{17}H_{19}N_3O_3$ $[M + H]^+$ m/z: 314.1499, found 314.1496.

3,5-Diethyl-N^1-(4-nitrophenyl)benzene-1,4-diamine (9c). Red oil, 12 mg, yield 4%, ^{1}H NMR (300 MHz, $CDCl_3$) δ: 1.26 (t, J_1 = 7.5 Hz, 6 H), 2.54 (q, J_1 = 7.5 Hz, 4 H), 3.69 (s, 2 H), 6.19 (s, 1 H), 6.72 (m, 2 H), 6.85 (s, 2 H), 8.06 (m, 2H). ^{13}C NMR (126 MHz, $CDCl_3$) δ: 152.5, 139.7, 138.4, 129.5, 128.8, 126.3, 122.3, 112.2, 24.2, 12.8. IR (KBr) ν (cm^{-1}): 3353, 2956, 2866, 1306. HRMS (ESI) calcd for $C_{16}H_{19}N_3O_2$ $[M + H]^+$ m/z: 286.1550, found 286.1564.

3,5-Dimethyl-N^1-(4-(trifluoromethyl)phenyl)benzene-1,4-diamine (9d). Colorless crystals, 50 mg, yield 18%, m.p. 115–117 °C, ^{1}H NMR (500 MHz, $CDCl_3$) δ: 2.18 (s, 6 H), 3.54 (brs, 2 H), 5.63 (brs, 1 H), 6.79 (d, J = 8.4 Hz, 2 H), 6.80 (s, 2 H), 7.38 (d, J = 8.4 Hz, 2 H). ^{13}C NMR (126 MHz, $CDCl_3$) δ: 149.4, 139.9, 130.9, 126.5 (q, J = 3.5 Hz), 124.9 (q, J = 270.4 Hz), 124.0, 122.8, 119.6 (q, J = 32.3 Hz), 113.3, 17.7. IR (KBr) ν (cm^{-1}): 3382, 2929, 2853, 1109. HRMS (ESI) calcd for $C_{15}H_{15}F_3N_2$ $[M + H]^+$ m/z: 281.1260, found 281.1274.

3-Ethyl-5-methyl-N^1-(4-(trifluoromethyl)phenyl)benzene-1,4-diamine (9e). Yellowish oil, 53 mg, yield 18%, ^{1}H NMR (300 MHz, $CDCl_3$) δ: 1.25 (t, J_1 = 7.5 Hz, 3 H), 2.18 (s, 3 H), 2.52 (q, J_1 = 7.5 Hz, 2 H), 3.60 (brs, 2 H), 5.65 (s, 1 H), 6.80 (d, J_2 = 8.4 Hz, 2 H), 6.81 (s, 2 H), 7.38 (d, J_2 = 8.4 Hz, 2H). ^{13}C NMR (126 MHz, $CDCl_3$) δ: 149.4, 139.3, 131.1, 128.6, 126.5 (d, J = 3.7 Hz), 124.9 (d, J = 270.4 Hz), 123.8, 123.1, 121.9, 119.6 (q, J = 32.4 Hz), 113.3, 24.2, 17.8, 13.0. IR (KBr) ν (cm^{-1}): 3385, 2934, 2873, 1110. HRMS (ESI) calcd for $C_{16}H_{17}F_3N_2$ $[M + H]^+$ m/z: 295.1417, found 295.1411.

3,5-Diethyl-N^1-(4-(trifluoromethyl)phenyl)benzene-1,4-diamine (9f). Yellow oil, 49 mg, yield 16%, ^{1}H NMR (300 MHz, $CDCl_3$) δ: 1.26 (t, J_1 = 7.5 Hz, 6 H), 2.54 (q, J_1 = 7.5 Hz, 4 H), 3.63 (brs, 2 H), 5.69 (s, 1 H), 6.82 (d, J_2 = 8.4 Hz, 2 H), 6.84 (s, 2 H), 7.39 (d, J_2 = 8.4 Hz, 2 H). ^{13}C NMR (126 MHz, $CDCl_3$) δ: 149.4, 138.7, 131.3, 128.9, 126.6 (q, J = 3.5 Hz), 124.9 (q, J = 270.3 Hz), 121.7, 119.7 (q, J = 33.1 Hz), 113.3, 24.3, 13.0. IR (KBr) ν (cm^{-1}): 3385, 2965, 2874, 1111. HRMS (ESI) calcd for $C_{17}H_{19}F_3N_2$ $[M + H]^+$ m/z: 309.1573, found 309.1572.

4-[(2-Amino-5-methylphenyl)amino]-3,5-dimethylbenzonitrile (15a). Pink crystals, 88 mg, yield 35%, m.p. 133–134 °C, ^{1}H NMR (300 MHz, $CDCl_3$) δ: 2.13 (s, 9 H), 3.65 (s, 2 H), 5.02 (s, 1 H), 6.17 (s, 1 H), 6.70 (s, 2 H), 7.36 (m, 2H). ^{13}C NMR (75 MHz, $CDCl_3$) δ: 145.5, 135.4, 132.5, 131.3, 131.2, 129.0, 123.7, 119.6, 119.3, 116.3, 105.4, 20.6, 18.5. IR (KBr) ν (cm^{-1}): 3459, 3365, 2924, 2855, 2220, 1601. HRMS (ESI) calcd for $C_{16}H_{17}N_3$ $[M + H]^+$ m/z: 252.1495, found 252.1502.

4-[(2-Amino-5-ethylphenyl)amino]-3-ethyl-5-methylbenzo-nitrile (15b). Pink oil, 45 mg, yield 16%, ^{1}H NMR (300 MHz, $CDCl_3$) δ: 1.07 (t, J_1 = 7.6 Hz, 3H), 1.17 (t, J_2 = 7.5 Hz, 3H), 2.08 (s, 3 H), 2.40 (q, J_1 = 7.6 Hz, 2H), 2.53 (q, J_2 = 7.5 Hz, 2H), 3.64 (s, 2 H), 5.10 (s, 1 H), 6.15 (s, 1 H), 6.68–6.75 (m, 2 H), 7.35 (s, 1 H), 7.39 (s, 1 H). ^{13}C NMR (75 MHz, $CDCl_3$) δ: 144.8, 137.3, 135.8, 135.2, 132.5, 132.1, 131.9, 130.5, 122.1, 119.7, 117.6, 116.4, 105.9, 28.1, 24.4, 18.6, 16.0, 13.8. IR (KBr) ν (cm^{-1}): 3366, 2964, 2917, 2871, 2849, 2221, 1599. HRMS (ESI) calcd for $C_{18}H_{21}N_3$ $[M + H]^+$ m/z: 280.1808, found 280.1814.

Typical procedure for the intercrossing experiments

A solution of *N*,*N*′-diaryl hydrazine **14a** (35 mg, 0.1 mmol), **14b** (38 mg, 0.1 mmol) [or **7a** (36 mg, 0.1 mmol), **7e** (39 mg, 0.1 mmol)], and conc. HCl (0.15 mL) in 10 mL of 95% ethanol was refluxed for 2 h under nitrogen. The reaction mixture was cooled to room temperature, neutralized with solid $NaHCO_3$, filtered, concentrated. The residue was subjected to the LC-MS analysis.

Typical procedure for the radical trapping experiments

A solution of *N*,*N*′-diaryl hydrazine **7d** (190 mg, 0.5 mmol) or **14a** (176 mg, 0.5 mmol), TEMPO (78 mg, 0.5 mmol, 2,2,6,6-

tetramethyl-1-piperidinyloxy, free radical), and conc. HCl (0.2 mL) in 10 mL of 95% ethanol was refluxed for 2 h under nitrogen. The reaction mixture was cooled to room temperature, neutralized with solid $NaHCO_3$, filtered, concentrated. The residue was purified by flash column chromatography on silica gel to afford **8d** (22% yield) and **9d** (17% yield), respectively, or 41 mg of **15a** as pink crystals in 33% yield.

Acknowledgements

This work was supported in part by The National Basic Research Program of China (no. 2013CB328905), the National Natural Science Foundation of China (Nos. 21372025 and 21172017) and specialized Research Fund for the Doctoral Program of Higher Education, Ministry of Education of China (no. 20110010110011). This paper is also supported by "Chemical Grid Project" of Beijing University of Chemical Technology.

Notes and references

1 B[1,3]-sigmatropic shift: (*a*) G. Zweifel and A. Horngy, *Synthesis*, 1973, 672; (*b*) K. G. Hancock and J. D. Kramer, *J. Am. Chem. Soc.*, 1973, **95**, 6463; (*c*) B. M. Miklailov, *Organomet. Chem. Rev., Sect. A*, 1972, **8**, 1; (*d*) G. W. Kramer and H. C. Brown, *J. Organomet. Chem.*, 1977, **132**, 9; (*e*) M. Biihl, P. R. Schleyer, M. A. Ibrahim and T. Clark, *J. Am. Chem. Soc.*, 1991, **113**, 2466; (*f*) U. Henriksen, J. P. Snyder and T. A. Halgren, *J. Org. Chem.*, 1981, **46**, 3767.

2 C[1,3]-sigmatropic shift: (*a*) R. W. Thies, *J. Am. Chem. Soc.*, 1972, **94**, 7074; (*b*) G. R. Krow and J. Reilly, *J. Am. Chem. Soc.*, 1975, **97**, 3837; (*c*) J. W. Lown, M. H. Akhtar and W. M. Dadson, *J. Org. Chem.*, 1975, **40**, 3363; (*d*) R. Fusco and F. Sannicolo, *Tetrahedron Lett.*, 1976, **17**, 3991; (*e*) R. W. Thies and E. P. Seitz, *J. Chem. Soc., Chem. Commun.*, 1976, 846; (*f*) S. Bartlett, R. D. Chambers and N. M. Kelly, *Tetrahedron Lett.*, 1980, **21**, 1891; (*g*) J. Barluenga, F. Aznar, R. Liz and M. Bayod, *J. Chem. Soc., Chem. Commun.*, 1984, 1427; (*h*) C. Bleasdale and D. W. Jones, *J. Chem. Soc., Chem. Commun.*, 1985, 1026; (*i*) M. E. Jung and S. M. Kaas, *Tetrahedron Lett.*, 1989, **30**, 641; (*j*) D. Desmaele and N. Champion, *Tetrahedron Lett.*, 1992, **33**, 4447; (*k*) B. Franzus, M. L. Scheinbaum, D. L. Waters and H. B. Bowlin, *J. Am. Chem. Soc.*, 1976, **98**, 1241; (*l*) K. Seki, W. Kiyokawa, H. Hashimoto, T. Uyehara, M. Ueno and T. Sato, *Chem. Lett.*, 1996, 1035; (*m*) F. X. Talamas, D. B. Smith, A. Cervantes, F. Franco, S. T. Cutler, D. G. Loughhead, D. J. Morgans Jr. and R. J. Weikert, *Tetrahedron Lett.*, 1997, **38**, 4725; (*n*) Y. L. Chen, C. K. Chang and N. C. Chang, *J. Chin. Chem. Soc.*, 1998, **45**, 649; (*o*) P. Bisel, G. Lauktien, E. Weckert and A. W. Frahm, *Tetrahedron: Asymmetry*, 1998, **9**, 4027; (*p*) J. D. Bender, P. A. Leber, R. R. Lirio and R. S. Smith, *J. Org. Chem.*, 2000, **65**, 5396; (*q*) J. E. Baldwin, *Chem. Rev.*, 2003, **103**, 1197; (*r*) P. Wipf, D. L. Waller and J. T. Reeves, *J. Org. Chem.*, 2005, **70**, 8096; (*s*) B. O. Ashburn, R. G. Carter and L. N. Zakharov, *J. Org. Chem.*, 2008, **73**, 7305.

3 Si[1,3]-sigmatropic shift: (*a*) K. Mach, F. Turecek, H. Antropiusova and V. Hanus, *Organometallics*, 1986, **5**, 1215; (*b*) M. T. Pereira, M. Pfeffer and M. A. Rotteveel, *J. Organomet. Chem.*, 1989, **375**, 139; (*c*) M. Takahashi and M. Kira, *J. Am. Chem. Soc.*, 1997, **119**, 1948; (*d*) M. Takahashi and M. Kira, *J. Am. Chem. Soc.*, 1999, **121**, 8597.

4 S[1,3]-sigmatropic shift: (*a*) K. Noerkjaer and A. Senning, *Chem. Ber.*, 1993, **126**, 73; (*b*) V. Ficeri, P. Kutschy, M. Dzurilla and J. Imrich, *Collect. Czech. Chem. Commun.*, 1994, **59**, 2650; (*c*) J. Maddaluno, O. Gaonach, A. Marcual, L. Toupet and G. P. Claude, *J. Org. Chem.*, 1996, **61**, 5290.

5 P[1,3]-sigmatropic shift: (*a*) K. Lammertsma, J. T. Hung, P. Chand and G. M. Gray, *J. Org. Chem.*, 1992, **57**, 6557; (*b*) B. Wang, C. H. Lake and K. Lammertsma, *J. Am. Chem. Soc.*, 1996, **118**, 1690.

6 (*a*) R. B. Woodward and R. Hoffmann, *The Conservation of Orbital Symmetry*, Verlag Chemie, Weinheim, 1970; (*b*) I. Fleming, *Frontier Orbitals and Organic Chemical Reactions*, Wiley-Interscience, New York, 1976.

7 S. L. Hou, X. Y. Li and J. X. Xu, *J. Org. Chem.*, 2012, **77**, 10856.

8 A. W. Hofmann, *Proc. R. Soc. London*, 1863, **12**, 576.

9 R. B. Carlin, R. G. Nelb and R. C. Odioso, *J. Am. Chem. Soc.*, 1951, **73**, 1002.

10 A different product ratio (2, 85% and 3, 15%) was reported by Shine and co-workers. See ref. 11f.

11 (*a*) M. J. S. Dewar, in *Molecular Rearrangement*, ed. P. de Mayo, Interscience, New York, 1969, vol. 1, pp. 323–343; (*b*) H. J. Shine, in *Mechanisms of Molecular Migrations*, ed. B. S. Thyagarajan, Interscience, New York, 1969, vol. 2, pp. 191–247; (*c*) H. J. Shine, in *Aromatic Rearrangement*, Elsevier, New York, 1967, pp. 126–179; (*d*) R. A. Cox and E. Buncel, in *The Chemistry of the Hydrazo, Azo, and Azoxy Groups*, ed. S. Patai, Wiley, New York, 1975, pp. 775–859; (*e*) D. V. Banthorpe, R. Bramley and J. A. Thomas, *J. Chem. Soc.*, 1964, 2864; (*f*) D. V. Banthorp, *Chem. Rev.*, 1970, **70**, 295; (*g*) G. A. Olah, K. Dunne, D. P. Kelly and Y. K. Mo, *J. Am. Chem. Soc.*, 1972, **94**, 7438; (*h*) J. D. Cheng and H. J. Shine, *J. Org. Chem.*, 1975, **40**, 703; (*i*) C. A. Bunton and R. J. Rubin, *J. Am. Chem. Soc.*, 1976, **98**, 4236; (*j*) A. Zhu-Ohlbach, R. Gleiter, R. Bleiter, H. L. Schmidt and T. Reda, *Eur. J. Org. Chem.*, 1998, 2409; (*k*) E. Buncel, *Can. J. Chem.*, 2000, **78**, 1251.

12 (*a*) H. J. Shine, *J. Phys. Org. Chem.*, 1989, **2**, 491 (review) (*b*) J. A. Berson, *J. Phys. Org. Chem.*, 2005, **18**, 572.

13 (*a*) H. J. Shine, G. N. Henderson, A. Schmid and P. Cu, *J. Am. Chem. Soc.*, 1977, **99**, 3719; (*b*) H. J. Shine, H. Zmuda, K. H. Park, H. Kwart, A. G. Horgan, C. Collins and B. E. Maxwell, *J. Am. Chem. Soc.*, 1981, **103**, 955; (*c*) H. J. Shine, H. Zmuda, K. H. Park, H. Kwart, A. G. Horgan and M. Brechbiel, *J. Am. Chem. Soc.*, 1982,

104, 2501; (*d*) H. J. Shine, K. H. Part, M. L. Brownawell and J. San Filippo Jr., *J. Am. Chem. Soc.*, 1984, **106**, 7007; (*e*) W. Subotkowski, L. Kupczy-Subotkowska and H. J. Shine, *J. Am. Chem. Soc.*, 1993, **115**, 5073.

14 (*a*) H. J. Shine, E. Gruszecka, W. Subotkowksi, M. Brownawell and J. San Fillipo Jr., *J. Am. Chem. Soc.*, 1985, **107**, 3218; (*b*) H. J. Shine, L. Kupczyk-Subotkowska and W. Subotkowski, *J. Am. Chem. Soc.*, 1985, **107**, 6674; (*c*) H. J. Shine, L. Kupczyk-Subotkowska and W. Subotkowski, *J. Am. Chem. Soc.*, 1987, **109**, 1286; (*d*) L. Kupczyk-Subotkowski, H. J. Shine, W. Subotkowski and J. Zygmunt, *Gazz. Chim. Ital.*, 1987, **117**, 513.

15 (*a*) H. J. Shine, H. Zmuda, H. Kwart, A. G. Horgan and M. Brechbiel, *J. Am. Chem. Soc.*, 1982, **104**, 5181; (*b*) E. S. Ree and H. J. Shine, *J. Am. Chem. Soc.*, 1986, **108**, 1000; (*c*) E. S. Ree and H. J. Shine, *J. Am. Chem. Soc.*, 1987, **109**, 5052; (*d*) E. S. Rhee and H. J. Shine, *J. Org. Chem.*, 1987, **52**, 5633; (*e*) H. J. Shine, in *Isotopes in Organic Chemistry*, ed. E. Buncel and W. H. Saunders Jr., Elsevier, Amsterdam, 1992, ch. 1, vol. 8.

16 S. Yamabe, H. Nakata and S. Yamazaki, *Org. Biomol. Chem.*, 2009, **7**, 4631.

17 G. Ghigo, S. Osella, A. Maranzana and G. Tonachini, *Eur. J. Org. Chem.*, 2011, 2326.

18 M. J. Smith and J. March, in *Advanced Organic Chemistry*, John Wiley & Sons, Hoboken, New Jersey, 2007, ch. 18–36, pp. 1678–1681.

19 K. Y. Kim, J. T. Shin, K. S. Lee and C. G. Cho, *Tetrahedron Lett.*, 2004, **45**, 117.

20 (*a*) J. Jacobson, *Justus Liebigs Ann. Chem.*, 1922, **428**, 76; (*b*) C. K. Ingold and H. W. Kidd, *J. Chem. Soc.*, 1933, 984.

21 M. J. Frisch, *et al.*, *Gaussian 09, Revision B.01*, Gaussian, Inc., Wallingford, CT, 2010.

22 (*a*) A. D. Becke, *J. Chem. Phys.*, 1993, **98**, 5648; (*b*) C. Lee, W. Yang and R. G. Parr, *Phys. Rev. B: Condens. Matter*, 1988, **37**, 785.

23 (*a*) V. Barone and M. Cossi, *J. Phys. Chem. A*, 1998, **102**, 1995; (*b*) M. Cossi, N. Rega, G. Scalmani and V. Barone, *J. Comput. Chem.*, 2003, **24**, 669; (*c*) Y. Takano and K. N. Houk, *J. Chem. Theory Comput.*, 2005, **1**, 70.

24 For recent examples of distortion/interaction analysis, see: (*a*) D. H. Ess and K. N. Houk, *J. Am. Chem. Soc.*, 2007, **129**, 10646; (*b*) D. H. Ess and K. N. Houk, *J. Am. Chem. Soc.*, 2008, **130**, 10187; (*c*) P. H.-Y. Cheong, R. S. Paton, S. M. Bronner, G.-Y. Im, N. K. Garg and K. N. Houk, *J. Am. Chem. Soc.*, 2010, **132**, 1267; (*d*) P. Liu, P. McCarren, P. H. Cheong, T. F. Jamison and K. N. Houk, *J. Am. Chem. Soc.*, 2010, **132**, 2050; (*e*) Y. Lan and K. N. Houk, *J. Am. Chem. Soc.*, 2010, **132**, 17921, and references cited therein.

25 Although slight carbon KIEs were observed in the rate-limiting step in the rearrangements: the phenomena have been found in the concerted 1,3-dipolar cycloaddition of *N*,α-diphenylnitrone and styrene with a carbon KIE ranging from 1.012 to 1.068 depending on which carbon atom was labelled (ref. 26), and the concerted [2 + 2] cycloaddition of diphenylketene and styrene with a carbon KIE in the range of 1.0055–1.08 (ref. 27).

26 B. M. Benjamin and C. J. Collins, *J. Am. Chem. Soc.*, 1973, **95**, 6145.

27 C. J. Collins, B. M. Benjamin and G. W. Kabalka, *J. Am. Chem. Soc.*, 1978, **100**, 2570.

28 For reviews, see: (*a*) S. E. Scheppele, *Chem. Rev.*, 1972, **72**, 511; (*b*) A. Maccoll, *Annu.Rep. Prog. Chem., Sect. A: Inorg. Phys. Chem.*, 1974, **71**, 77 For examples, see; (*c*) J. Bron and J. B. Stothers, *Can. J. Chem.*, 1968, **46**, 1435; (*d*) J. Bron and J. B. Stothers, *Can. J. Chem.*, 1969, **47**, 2506.